



The following Communications have been judged by at least two referees to be “very important papers” and will be published online at www.angewandte.org soon:

T. Lewis, M. Faubel, B. Winter, J. C. Hemminger*

CO₂ Capture in an Aqueous Solution of an Amine: Role of the Solution Interface

Y. H. Kim, S. Banta*

Complete Oxidation of Methanol in an Enzymatic Biofuel Cell by a Self-Assembling Hydrogel Created from Three Modified Dehydrogenases

L. Furst, J. M. R. Narayanan, C. R. J. Stephenson*

Total Synthesis of (+)-Gliocladin C Enabled by Visible-Light Photoredox Catalysis

P. Höhn,* F. Jach, B. Karabiyik, S. Agrestini, F. R. Wagner, M. Ruck, L. H. Tjeng, R. Kniep*

Highly Reduced Cobaltates Sr₃[Co(CN)₃] and Ba₃[Co(CN)₃]: Crystal Structure, Chemical Bonding, and Conceptional Considerations

R. M. Culik, A. L. Serrano, M. R. Bunagan,* F. Gai*

Achieving Secondary Structural Resolution in Kinetic Measurements of Protein Folding: A Case Study of the Folding Mechanism of Trp-cage

C.-Y. Chang, C.-E. Wu, S.-Y. Chen, C. Cui, Y.-J. Cheng, C.-S. Hsu,* Y.-L. Wang,* Y. Li

Enhanced Performance and Stability of a Polymer Solar Cell by Incorporating Vertically Aligned, Cross-Linked Fullerene Nanorods

L. P. Hansen, Q. M. Ramasse, C. Kisielowski, M. Brorson, E. Johnson, H. Topsøe, S. Helveg

Atomic-Scale Edge Structures on Industrial MoS₂ Nanocatalysts

J. Huber, B. Scheinhardt, T. Geldhauser, J. Boneberg, S. Mecking*

Laser-Interference Patterning of Polymerization Catalysts



“What I look for first in a publication is architecturally beautiful structures.

My favorite piece of research is R. B. Woodward’s total synthesis of reserpine ...”

This and more about Masayuki Inoue can be found on page 9016.

Author Profile

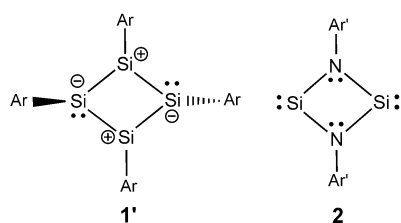
Masayuki Inoue _____ 9016

Handbook of Fluorescence Spectroscopy and Imaging

Markus Sauer, Johan Hofkens, Jörg Enderlein

Books

reviewed by M. Levitus _____ 9017



Ar = novel bulky aryl group
Ar' = Power-type terphenyl group

The fundamental question of how silicon handles antiaromaticity in four-membered ring systems has been answered by the synthesis and characterization of the first tetrasilacyclobutadiene Si₄Ar₄ (**1**) and by the first dimeric silaisonitrile Si₂(NAr')₂ (**2**). Compound **1** is best described by the charge-separated resonance structure **1'** and **2** by a structure with π-type lone pairs at the nitrogen atoms and vacant π orbitals at the silicon atoms.

Highlights

Silicon Chemistry

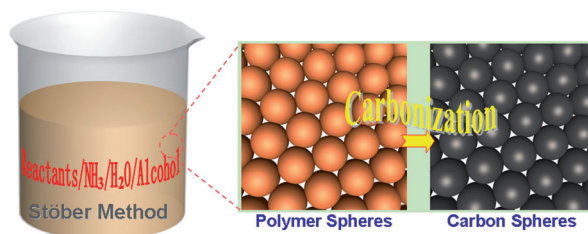
P. Jutzi* _____ 9020–9022

Low-Valent Silicon in Formally Antiaromatic Four-Membered Ring Systems

Colloidal Spheres

A.-H. Lu,* G.-P. Hao,
Q. Sun _____ 9023–9025

Can Carbon Spheres Be Created through
the Stöber Method?



The Stöber method is an authoritative approach for the synthesis of monodisperse colloidal silica spheres; this method

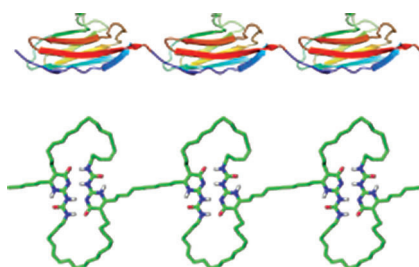
has now been extended to the synthesis of monodisperse resorcinol-formaldehyde resin polymer and carbon spheres.

Reviews

Biomimetic Materials

A. M. Kushner, Z. Guan* _____ 9026–9057

Modular Design in Natural and
Biomimetic Soft Materials



Nature's bounty: Recent advances in analytical and synthetic tools are facilitating the development of materials inspired by nature. This Review highlights the history and the state-of-the-art in the quest to understand the molecular mechanisms behind nature's most remarkable peptide-based materials, as well as the attempts to apply that understanding to design biomimetic materials.

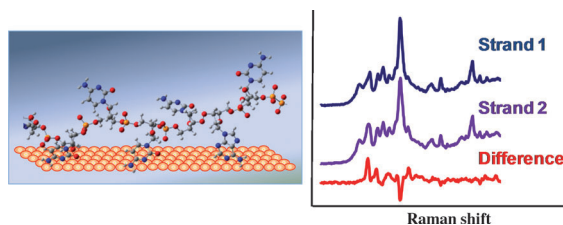
Communications

DNA Analysis

E. Papadopoulou,
S. E. J. Bell* _____ 9058–9061



Label-Free Detection of Single-Base
Mismatches in DNA by Surface-Enhanced
Raman Spectroscopy



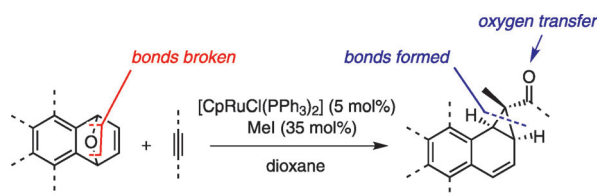
Singles only: DNA sequences can be induced to spontaneously adsorb to the surfaces of Ag colloids through their nucleotide side chains (see picture). The SERS spectra of these nonspecifically bound strands are sufficiently reproducible that they can be used to identify single-

base mismatches in short (25-mer and 23-mer) strands. Subtracting the spectra of different DNA sequences results in difference spectra that contain features corresponding to the exchanged nucleotides.

For the USA and Canada:
ANGEWANDTE CHEMIE International
Edition (ISSN 1433-7851) is published weekly
by Wiley-VCH, PO Box 191161, 69451 Wein-
heim, Germany. Air freight and mailing in the
USA by Publications Expediting Inc., 200
Meacham Ave., Elmont, NY 11003. Periodicals

postage paid at Jamaica, NY 11431. US POST-
MASTER: send address changes to *Angewandte
Chemie*, Journal Customer Services, John
Wiley & Sons Inc., 350 Main St., Malden,
MA 02148-5020. Annual subscription price for
institutions: US\$ 11,738/10,206 (valid for print
and electronic / print or electronic delivery); for

individuals who are personal members of a
national chemical society prices are available
on request. Postage and handling charges
included. All prices are subject to local VAT/
sales tax.



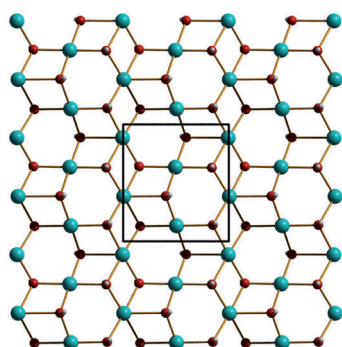
Stereodefined: The title reaction provides an atom-economic route to benzonorcaradienes. The diastereoselectivity of the coupling relies upon the structure of the alkene; unsubstituted bicyclic alkenes

afforded exclusively *exo*-benzonorcaradienes (see scheme) whereas the bicyclic alkenes with substituents at the bridge-head positions resulted in *endo*-benzonorcaradienes.

Ruthenium Catalysis

A. Tenaglia,* S. Marc, L. Giordano,
I. De Riggi _____ 9062–9065

Ruthenium-Catalyzed Coupling of Oxabenzonorbornadienes with Alkynes Bearing a Propargylic Oxygen Atom: Access to Stereodefined Benzonorcaradienes



Cationic layers: Copper hydroxide ethanedisulfonate consists of cationic sheets (see structure of a $[\text{Cu}_4(\text{OH})_6]^{2+}$ layer; Cu green, O red, H white) with ethanedisulfonate as extraframework counteranion. This material shows excellent anion exchange properties for both organics and metal oxo anion pollutants, with over five times higher adsorption capacity for permanganate than hydrotalcite.

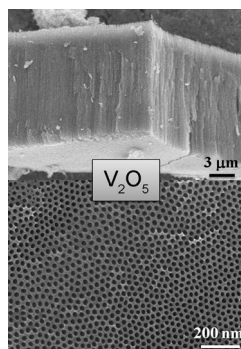
Layered Compounds

H. Fei, S. R. J. Oliver* _____ 9066–9070

Copper Hydroxide Ethanedisulfonate: A Cationic Inorganic Layered Material for High-Capacity Anion Exchange



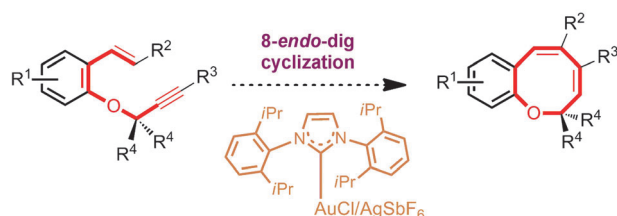
Vanadium oxide layers with homogeneous nanoporous nanotubular morphology (see picture) were successfully fabricated by direct anodization of vanadium in fluoride electrolytes such as $[\text{TiF}_6]^{2-}$ or $[\text{BF}_4]^-$. The pore size and layer thickness can easily be controlled by tailoring the electrochemical conditions. Such nanotubular or porous structures are promising for the fabrication of lithium-ion insertion electrodes.



Metal Oxides

Y. Yang, S. P. Albu, D. Kim,
P. Schmuki* _____ 9071–9075

Enabling the Anodic Growth of Highly Ordered V_2O_5 Nanoporous/Nanotubular Structures



A golden dig! Gold-catalyzed direct access to functionalized 2*H*-1-benzoxocines, eight-membered-ring ethers, is described.

This unprecedented synthesis of benzoxocines occurs by an 8-*endo*-dig cyclization of the 1,7-enyne substrates.

Gold Catalysis

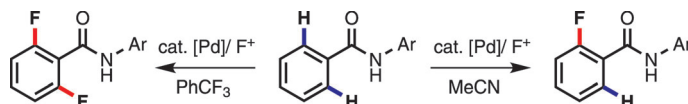
K. Wittstein, K. Kumar,*
H. Waldmann* _____ 9076–9080

Gold(I)-Catalyzed Synthesis of Benzoxocines by an 8-*endo*-dig Cyclization



C–H Fluorination

K. S. L. Chan, M. Wasa, X. Wang,
J.-Q. Yu* 9081 – 9084



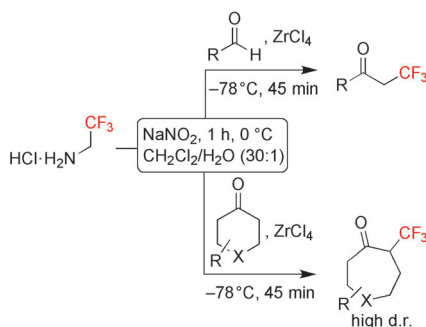
Finally, a choice! A highly selective palladium(II)-catalyzed *ortho*-monofluorination reaction has been achieved for the first time through a weak coordination (see scheme; Ar = 2,3,5,6-tetrafluoro-4-(trifluoromethyl)phenyl). Simple modification

of this protocol allows for a choice between mono- and difluorination. The mono- and difluorinated benzoic acid derivatives are valuable in the pharmaceutical and agrochemical industries.

Synthetic Methods

B. Morandi, E. M. Carreira* 9085 – 9088

Synthesis of Trifluoroethyl-Substituted Ketones from Aldehydes and Cyclohexanones

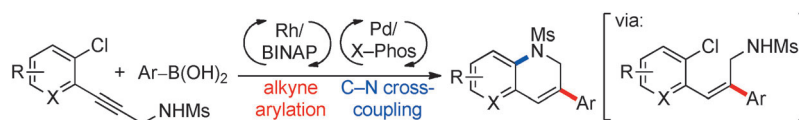


A trifluoromethylated symphony! A new transformation involving trifluoromethyl diazomethane generated in situ has been developed that allows direct access to trifluoroethyl ketone derivatives from aldehyde and cyclohexanone compounds (see scheme).

Multicatalytic Reactions

J. Pantelev, L. Zhang,
M. Lautens* 9089 – 9092

Domino Rhodium-Catalyzed Alkyne Arylation/Palladium-Catalyzed N Arylation: A Mechanistic Investigation



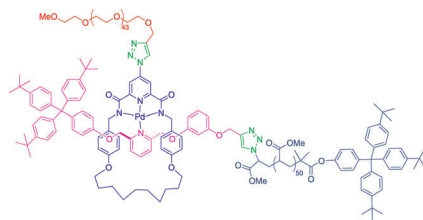
It takes two to tango: A domino multicatalytic synthesis of dihydroquinolines is realized, wherein the products of a rhodium-catalyzed arylation of alkynes are cyclized by a palladium-promoted C–N

cross-coupling (see scheme). The combination of catalysts with potentially exchangeable ligands is remarkable as each metal–ligand combination affords specific reactivity and selectivity.

Polymer Architectures

G. De Bo, J. De Winter, P. Gerbaux,
C. A. Fustin* 9093 – 9096

Rotaxane-Based Mechanically Linked Block Copolymers

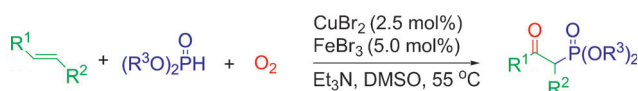


We just clicked: A convergent approach consisting of two successive copper(I)-catalyzed azide–alkyne cycloaddition “click” reactions leads to a diblock copolymer in which the two blocks are linked by a rotaxane-type mechanical bond (see scheme). Rotaxane formation is templated by a square-planar Pd^{II} complex.

Synthetic Methods

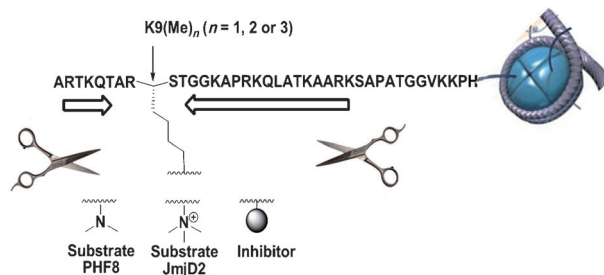
W. Wei, J.-X. Ji* 9097 – 9099

Catalytic and Direct Oxyphosphorylation of Alkenes with Dioxigen and H-Phosponates Leading to β-Ketophosphonates



Direct access: The title reaction has been developed under mild reaction conditions (see scheme; DMSO = dimethyl sulfoxide). This reaction can be effectively scaled up and offers not only a green and

attractive approach to β-ketophosphonates, but also a useful example of direct incorporation of an oxygen atom from dioxigen into organic frameworks.



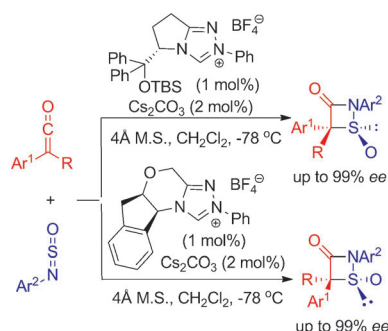
How low can you go? The natural substrate for the epigenetic regulators PHF8, JmjD2A, and JmjD2C (lysine demethylases), a peptide consisting of 39 amino acid residues, can be truncated to 14, 8, and 4 amino acids, respectively, while

maintaining catalytic activity (see picture). Inhibitors were prepared by attaching small molecules to the truncated substrates. Selective inhibition of JmjD2C over JmjD2A and PHF8 was possible.

Inhibitors

B. Lohse, A. L. Nielsen, J. B. L. Kristensen, C. Helgstrand, P. A. C. Cloos, L. Olsen, M. Gajhede, R. P. Clausen,*
J. L. Kristensen* _____ 9100–9103

Targeting Histone Lysine Demethylases by Truncating the Histone 3 Tail to Obtain Selective Substrate-Based Inhibitors

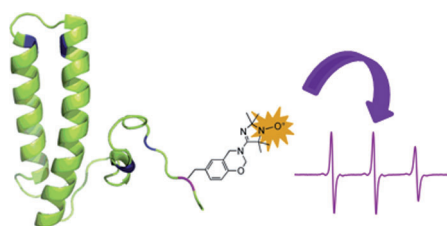


Sultam of swing: Both enantiomers of 1,2-thiazetidin-3-one oxides were obtained in very good yields with excellent enantioselectivities when using N-heterocyclic carbene catalysts (see scheme; M.S. = molecular sieves, TBS = *tert*-butyldimethylsilyl). The products were easily converted into 3-oxo- β -sultams, α -mercapto amides, and β -mercapto amines through oxidation or reduction.

Asymmetric Catalysis

T.-Y. Jian, L. He, C. Tang, S. Ye* _____ 9104–9107

N-Heterocyclic Carbene Catalysis: Enantioselective Formal [2+2] Cycloaddition of Ketenes and N-Sulfinylanilines



Keeping tabs on tyrosine: A three-component Mannich-type reaction extends the scope of site-directed spin labeling by selectively labeling the unique tyrosine residue of CP12 protein (see picture), as

was confirmed by mass spectrometry. EPR spectroscopy of the labeled protein showed a very high mobility of the probe, which remained very mobile after complex formation with GAPDH.

Protein Labeling

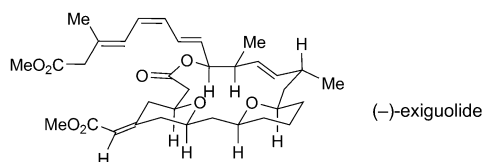
M. Lorenzi, C. Puppo, R. Lebrun, S. Lignon, V. Roubaud, M. Martinho, E. Mileo, P. Tordo, S. R. A. Marque,*
B. Gontero, B. Guigliarelli, V. Belle* _____ 9108–9111

Tyrosine-Targeted Spin Labeling and EPR Spectroscopy: An Alternative Strategy for Studying Structural Transitions in Proteins



Total Synthesis

E. A. Crane, T. P. Zabawa, R. L. Farmer,
K. A. Scheidt* _____ 9112–9115



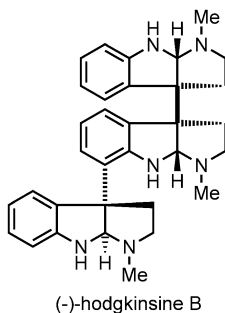
Enantioselective Synthesis of
(-)-Exiguolide by Iterative Stereoselective
Dioxinone-Directed Prins Cyclizations

Three become one: The title compound can be prepared in 26 steps by employing a unified Prins cyclization strategy to construct both tetrahydropyran rings (see scheme). The route combines two similar dioxinone fragments and one aldehyde

component to generate the core structure. (-)-Exiguolide selectively inhibits the growth of A549 cancer cells at low concentrations; the triene side chain and the Z-enoate geometry are both necessary for this cytotoxicity.

Alkaloid Synthesis

R. H. Snell, R. L. Woodward,
M. C. Willis* _____ 9116–9119

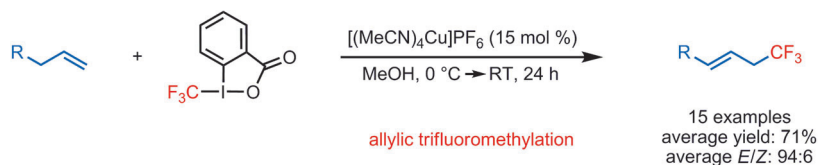


Catalytic Enantioselective Total Synthesis
of Hodgkinsine B

The power of palladium: The total synthesis of the alkaloid hodgkinsine B has been achieved with just six isolated intermediates and only four chromatographic operations. The route involves a palladium-catalyzed enantioselective desymmetrizing N-allylation of *meso*-chimonanthine to establish the absolute configuration and elaboration of the desymmetrized core by a diastereoselective palladium-catalyzed α -oxindole arylation.

Trifluoromethylation

A. T. Parsons,
S. L. Buchwald* _____ 9120–9123



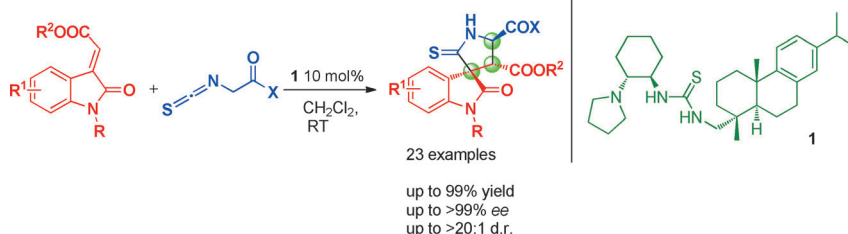
Copper-Catalyzed Trifluoromethylation of
Unactivated Olefins

Activating the inactive: A copper-catalyzed allylic trifluoromethylation of unactivated terminal olefins proceeds under mild conditions to produce linear allylic trifluoromethylated products with high

E/Z selectivity (see scheme). The reaction can be applied to a range of substrates bearing numerous functional groups. Furthermore, the reaction is scalable and amenable to a benchtop setup.

Asymmetric Synthesis

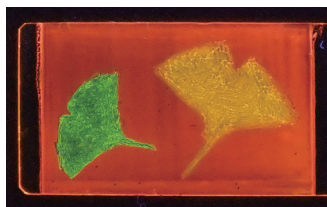
Y.-M. Cao, X.-X. Jiang, L.-P. Liu, F.-F. Shen,
F.-T. Zhang, R. Wang* _____ 9124–9127



Enantioselective Michael/Cyclization
Reaction Sequence: Scaffold-Inspired
Synthesis of Spirooxindoles with Multiple
Stereocenters

A-spiro-ing: The title reaction of α -isothiocyanato imides and methyleneindolinones has been realized for the first time using **1** as the catalyst. This newly developed synthetic method provides a simple,

efficient, and environmentally friendly way to access, in an enantioselective manner, densely functionalized spirooxindoles having three contiguous stereogenic centers.

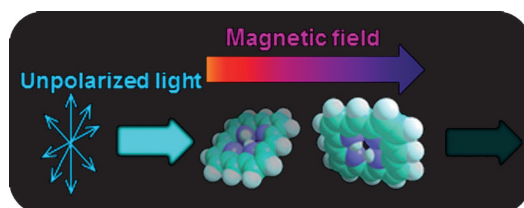


A glowing image: The photoluminescent colors reddish-orange, yellow, and green, are generated from a single liquid-crystalline mixture containing one lumino-phore (see picture). The colors are easily distinguished by the naked eye and can be reversibly written and erased. Moreover, these luminescent colors can be switched by mechanical and thermal stimuli.

Materials Chemistry

Y. Sagara, T. Kato* — 9128–9132

Brightly Tricolored Mechanochromic Luminescence from a Single-Lumino-phore Liquid Crystal: Reversible Writing and Erasing of Images



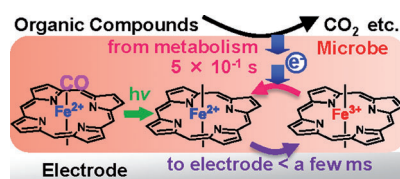
Direction decides: Magneto-chiral dichroism describes the dependence of the absorbance of a chiral molecule on the direction of a magnetic field to which it is

exposed, and it may help to explain the homochirality of life. This phenomenon was now observed in organic compounds using porphyrin J-aggregates.

Chirality

Y. Kitagawa, H. Segawa, K. Ishii* — 9133–9136

Magneto-Chiral Dichroism of Organic Compounds

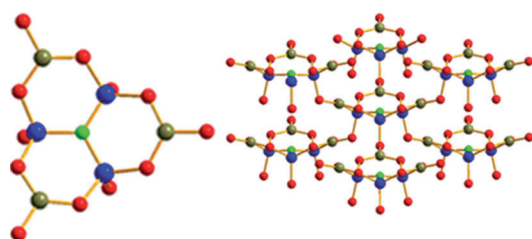


Morning light: In vivo photodissociation of CO from bacterial *c*-type cytochromes yields a redox-active Fe²⁺ form, which can be oxidized at an electrode surface to the Fe³⁺ form. Reduction by electrons from the metabolic pathway regenerates the Fe²⁺ form (see picture). Spectroscopic monitoring of this process yields information on the in vivo respiratory electron-transport dynamics.

In Vivo Electron Transport

T. Shibamura, R. Nakamura, Y. Hirakawa, K. Hashimoto,* K. Ishii* — 9137–9140

Observation of In Vivo Cytochrome-Based Electron-Transport Dynamics Using Time-Resolved Evanescent Wave Electroabsorption Spectroscopy



Structure matters: Owing to the structure and arrangement of the [Be₃B₃O₁₂F]¹⁰⁻ group (see picture, left, Be blue, B olive, F green, O red), the mixed-cation fluorine beryllium borate NaSr₃Be₃B₃O₉F₄ (right)

exhibits a large second harmonic generation effect and a short UV absorption edge. Its crystals show no layering tendency, making it promising for applications in deep-UV nonlinear optics.

Structure–Property Relationships

H. Huang, J. Yao, Z. Lin, X. Wang, R. He, W. Yao, N. Zhai, C. Chen* — 9141–9144

NaSr₃Be₃B₃O₉F₄: A Promising Deep-Ultraviolet Nonlinear Optical Material Resulting from the Cooperative Alignment of the [Be₃B₃O₁₂F]¹⁰⁻ Anionic Group

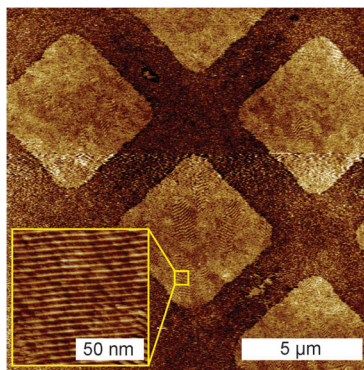


DNA Crystal Growth

J. Lee, S. Kim, J. Kim, C.-W. Lee, Y. Roh,*
S. H. Park* ————— 9145–9149



Coverage Control of DNA Crystals Grown by Silica Assistance



A surface-assisted fabrication scheme enables direct surface coverage control of functionalized DNA nanostructures on centimeter-scaled silica (SiO₂) substrates from 0 to 100% (see picture). Electrostatic interactions between the DNA structures and the surface lead to dramatic topological changes of the structures, thereby creating novel formations of the crystals.

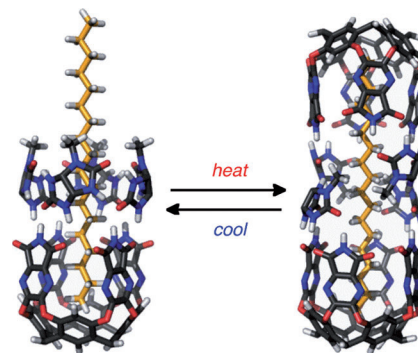
Self-Assembly

Y. Yamauchi, D. Ajami, J.-Y. Lee,
J. Rebek, Jr.* ————— 9150–9153



Deconstruction of Capsules Using Chiral Spacers

Interconvertible host: Extended cavitands and capsules that recognize *n*-alkanes were generated using *N*-methyl glycoluril as a chiral spacer. The two host assemblies were interconverted by factors such as temperature, concentration, and guest length (see scheme).



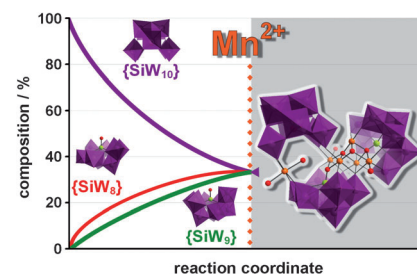
Polyoxometalates

S. G. Mitchell, P. I. Molina, S. Khanra,
H. N. Miras, A. Prescimone,
G. J. T. Cooper, R. S. Winter, E. K. Brechin,
D.-L. Long, R. J. Cogdell,
L. Cronin* ————— 9154–9157



A Mixed-Valence Manganese Cubane Trapped by Inequivalent Trilacunary Polyoxometalate Ligands

Three's a charm: The title compound (see picture, right, WO₆ purple polyhedra, Mn orange and brown, Si green, O red) contains an embedded mixed-valence {Mn₅O₆} cubane core, which is structurally similar to the active site in photosystem II. Solid-, solution-, and gas-phase studies indicate the presence of three lacunary Keggin fragments, thereby giving insight into the complex solution chemistry of plenary POM fragments.

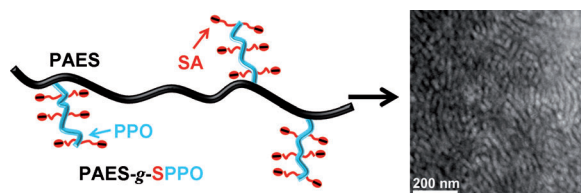


Materials Science

N. Li, C. Wang, S. Y. Lee, C. H. Park,
Y. M. Lee,* M. D. Guiver* — 9158–9161

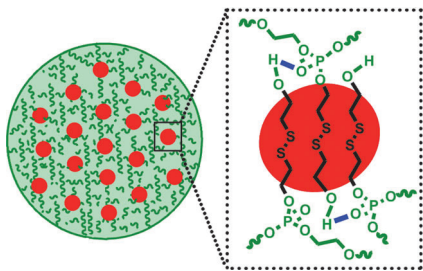


Enhancement of Proton Transport by Nanochannels in Comb-Shaped Copoly(arylene ether sulfone)s



Combed to perfection: Fully aromatic comb-shaped copolymers based on a poly(arylene ether sulfone) (PAES) backbone with highly sulfonated (SA) poly(phenylene oxide) (PPO) graft chains have a nanochannel morphology (see picture)

for efficient proton transport. These molecular structures show a dramatic enhancement in proton conductivity under partially hydrated conditions compared with typical hydrocarbon polymer electrolytes.

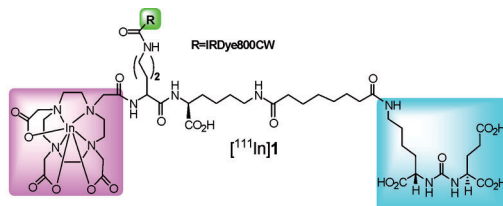
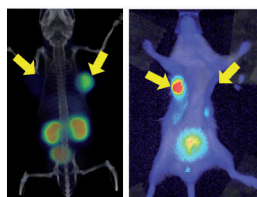


The best of both worlds: A novel amphiphilic homopolymer synthesized from a monomer consisting of a hydrophobic group (see picture, red) and a hydrophilic moiety (green) self-assembles in aqueous solution. The resulting micelles have a multi-core/shell structure and exhibit smart redox-responsive properties, thus providing a favorable drug delivery platform for cancer therapy.

Polymer Self-Assembly

J. Y. Liu, W. Huang,* Y. Pang, P. Huang, X. Y. Zhu, Y. F. Zhou, D. Y. Yan* _____ 9162–9166

Molecular Self-Assembly of a Homopolymer: An Alternative To Fabricate Drug-Delivery Platforms for Cancer Therapy



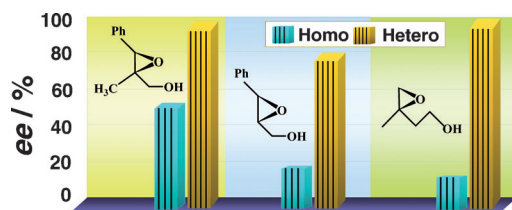
One reagent for two techniques: Compound $[^{111}\text{In}]1$ provides a platform for sequential radionuclide and optical imaging of prostate cancer through targeting of the prostate-specific membrane antigen.

Because the same subject can be dual-imaged after one injection of the agent, these findings support rapid clinical translation.

Dual-Modality Imaging Agents

S. R. Banerjee, M. Pullambhatla, Y. Byun, S. Nimmagadda, C. A. Foss, G. Green, J. J. Fox, S. E. Lupold, R. C. Mease, M. G. Pomper* _____ 9167–9170

Sequential SPECT and Optical Imaging of Experimental Models of Prostate Cancer with a Dual-Modality Inhibitor of the Prostate-Specific Membrane Antigen



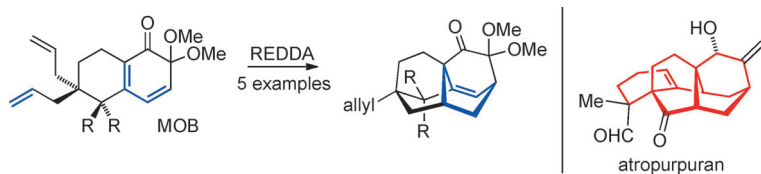
Layered catalyst: The attachment of α -amino acid ligands to inorganic nanosheets for use as ligands to vanadium, resulted in a catalyst that enhanced the enantioselectivity of the epoxidation of allylic alcohols (see picture). The catalyst

can be colloidized, allowing for the catalytic reactions to be carried out under pseudo-homogeneous reaction conditions and also the catalysts to be directly recycled by simple liquid/liquid separation.

Synthetic Methods

J. Wang, L. Zhao, H. Shi, J. He* _____ 9171–9176

Highly Enantioselective and Efficient Asymmetric Epoxidation Catalysts: Inorganic Nanosheets Modified with α -Amino Acids as Ligands



Masked talent: A tetracyclo-[5.3.3.0^{4,9}.0^{4,12}]tridecane skeleton can be accessed by an intramolecular reverse-electron-demand Diels–Alder (REDDA) reaction of masked *ortho*-benzoquinone

(MOB; see scheme). This reaction gives access to the pentacyclic framework of atropurpuran, and also enables the construction of other anti-Bredt and cage-like complex molecules.

Natural Product Synthesis

T. Suzuki, A. Sasaki, N. Egashira, S. Kobayashi* _____ 9177–9179

A Synthetic Study of Atropurpuran: Construction of a Pentacyclic Framework by an Intramolecular Reverse-Electron-Demand Diels–Alder Reaction

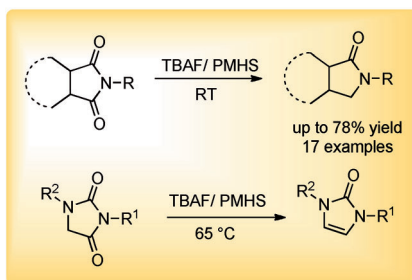


Chemoselective Reduction

S. Das, D. Addis, L. R. Knöpke,
U. Bentrup, K. Junge, A. Brückner,
M. Beller* _____ 9180–9184



Selective Catalytic Monoreduction of
Phthalimides and Imidazolidine-2,4-
diones



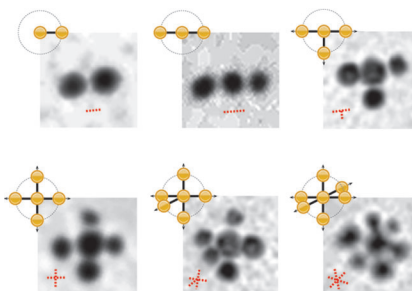
Fluoride's new role: Selective and efficient monoreductions of imides can be achieved with polymethylhydrosiloxane (PMHS) and tetra-*n*-butylammonium fluoride (TBAF) as catalyst (see scheme). The system is characterized by good chemoselectivity, operational simplicity, and functional-group tolerance; a concise mechanistic proposal was possible from in situ spectroscopic investigations.

Self-Assembly

J.-W. Kim,* J.-H. Kim,
R. Deaton _____ 9185–9190



DNA-Linked Nanoparticle Building Blocks
for Programmable Matter



One step at a time: DNA linkers were placed at defined locations and in defined 3D orientations on a colloidal nanoparticle. Because the implemented ligand-replacement strategy was carried out sequentially, DNA linkers maximally segregated, producing a nanoparticle with linkers at 90 or 180° angles (see picture). These building blocks should enable assembly of anisotropic nanostructures with precisely designed geometry and complex functionality.

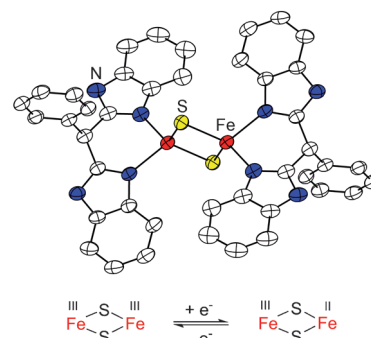
Iron–Sulfur Clusters

A. Albers, S. Demeshko, S. Dechert, E. Bill,
E. Bothe, F. Meyer* _____ 9191–9194



The Complete Characterization of a
Reduced Biomimetic [2 Fe–2 S] Cluster

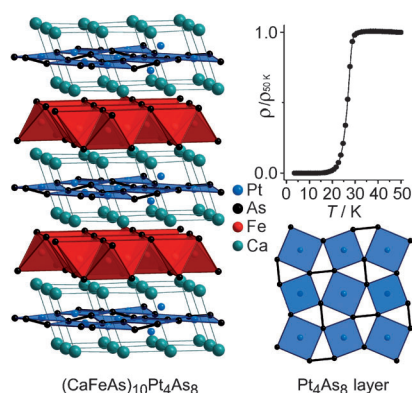
Cores and effect: A biomimetic [2 Fe–2 S] cluster is characterized crystallographically in both the [Fe^{III}Fe^{III}] and the mixed-valent [Fe^{III}Fe^{II}] forms—the [2 Fe–2 S] cores show only minor geometric differences. The reduced form has an *S* = 1/2 ground state and the unpaired electron is partially delocalized over the cluster core. The experimental effective coupling constant predicts the position of the intervalence charge transfer band in the IR regime.



Superconductors

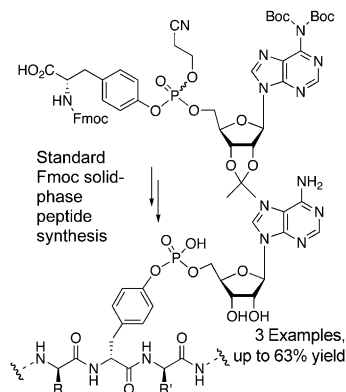
C. Löhnert, T. Stürzer, M. Tegel,
R. Frankovsky, G. Friederichs,
D. Johrendt* _____ 9195–9199

Superconductivity up to 35 K in the Iron
Platinum Arsenides
(CaFe_{1-x}Pt_xAs)₁₀Pt_{4-y}As₈ with Layered
Structures



The family of iron arsenide superconductors is expanded by the new iron platinum compounds (CaFe_{1-x}Pt_xAs₁₀)Pt_{4-y}As₈ with novel crystal structures. Layers of FeAs_{4/4} tetrahedra and of nearly planar PtAs_{4/2} squares with (As₂)⁴⁻ dumbbells are stacked in different ways, resulting in polytypes with triclinic or tetragonal symmetry. Superconductivity up to 35 K is induced either by Pt doping of the Fe site or by electron transfer from PtAs to FeAs layers.

The enzyme DrrA of the human pathogen *Legionella pneumophila* adenylylates specifically a tyrosine of the GTPase Rab1. An efficient synthesis route using Fmoc solid phase peptide synthesis led to Tyr-adenylylated peptides and allowed the generation of mono-selective polyclonal antibodies against this post-translational modification.

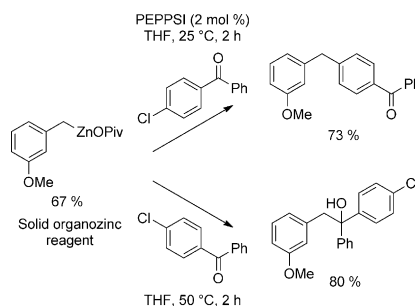


Post-Translational Modification

C. Smit, J. Blümer, M. F. Eerland, M. F. Albers, M. P. Müller, R. S. Goody, A. Itzen,* C. Hedberg* — 9200–9204

Efficient Synthesis and Applications of Peptides containing Adenylylated Tyrosine Residues

Powdered organozinc reagents: Various aryl and heteroaryl bromides as well as benzylic chlorides react with Mg and Zn(OPiv)₂·2 LiCl (OPiv = pivalate) to provide solid organozinc reagents after solvent evaporation. These powders can be stored at room temperature under argon for months and can be manipulated in air for a short time. They undergo smooth Negishi cross-coupling and carbonyl addition reactions (see scheme).



Organozinc Reagents

S. Bernhardt, G. Manolikakes, T. Kunz, P. Knochel* — 9205–9209

Preparation of Solid Salt-Stabilized Functionalized Organozinc Compounds and their Application to Cross-Coupling and Carbonyl Addition Reactions



Supporting information is available on www.angewandte.org (see article for access details).



A video clip is available as Supporting Information on www.angewandte.org (see article for access details).



This article is available online free of charge (Open Access)

Looking for outstanding employees?

Do you need another expert for your excellent team?
... Chemists, PhD Students, Managers, Professors, Sales Representatives...
Place an advert in the printed version and have it made available online for 1 month, free of charge!

Angewandte Chemie International Edition

Advertising Sales Department: Marion Schulz

Phone: 0 62 01 - 60 65 65

Fax: 0 62 01 - 60 65 50

E-Mail: MSchulz@wiley-vch.de

Service

Spotlight on Angewandte's
Sister Journals — 9010–9012

Preview — 9211